JOURNAL OF AIRCRAFT
Vol. 46, No. 4, July–August 2009

Catastrophe Model for Supersonic Inlet Start/Unstart

Cui Tao,* Yu Daren,† Chang Juntao,‡ and Bao Wen§
Harbin Institute of Technology, 150001 Heilongjiang, People's Republic of China

DOI: 10.2514/1.38926

Mathematical models may be very valuable for studying the flow laws of supersonic inlet start/unstart. From a viewpoint of structure stability, this paper makes a link between the catastrophe points of inlet start/unstart and the singular points in Whitney's singularity theory, from which we take notice of the conception of singularity classification, which may be helpful for modeling the catastrophe points of inlet start/unstart. By further research, Thom's catastrophe theory is found to be the right mathematical tool to classify general singularities by topological method. This paper makes an effort to model the catastrophe points of inlet start/unstart by the elementary catastrophe model in catastrophe theory and puts forward a new method to fit data to the catastrophe model. The method is based on nonlinear topological transformation, which has provided an improvement over the existing Cobb's method. Simulation results have shown that the present model is in good agreement with the data.

Nomenclature

M	=	Mach number
u	=	independent variable
V	=	potential function
x	=	dependent variable
α	=	angle of attack
γ	=	weight coefficient
θ	=	weight coefficient
λ	=	the location parameter
σ	=	scale parameter
Φ	=	mass-flow-rate coefficient

Subscripts

0	=	incoming flow

I. Introduction

STARTING a supersonic inlet of such airbreathing propulsion systems as ramjet and scramjet engines can be a very complex process that is influenced by a variety of aerodynamic phenomena. Inlet starting is defined as the ingestion of normal shock trains from the front of the inlet through the inlet throat to a point downstream of the throat. This can be a very unstable condition, and the slightest perturbation can cause the normal shock trains to be ejected from the inlet (i.e., inlet unstart). Inlet unstart is detrimental to engine performance because it severely increases drag, does not pass the necessary mass flow, and spills compressed air. In some conditions, it may even cause catastrophic damage during supersonic flight. Therefore, it is necessary to study the flow phenomena that occur during inlet start/unstart. Over the past decades, many investigations have been conducted to examine the mechanisms of inlet start/unstart. Mayer and Paynter [1,2] simulated an axisymmetric inlet unstart due to the variation of freestream variables such as temperature, velocity, and pressure. Neaves et al. [3] simulated the 3-D inlet unstart caused by a combustor perturbation. Zha et al. [4,5] investigated the unstart transient mechanism of a typical axisymmetric inlet at different angles of attack. Cox et al. [6] presented several mechanisms of supersonic inlet unstart, including backpressure unstart, overcontraction unstart, and the angle-of-attack unstart. Schmitz and Bissinger [7] and Van Wie and Kwok [8] analyzed the major factors that influence the inlet operation mode and studied the start/unstart characteristic of 2-D supersonic inlet. Reinartz and Herrmann [9] and Emami and Trexler [10] studied the variation of isolator geometry and its influence on the overall inlet compression efficiency; the investigations show that the sustainable backpressure is strongly influenced by the isolator length.

The significant amount of numerical and experimental studies have aimed at understanding the unstart mechanism and, further, holding the flow laws of inlet start/unstart due to the variation of freestream and downstream variables, such as flight Mach number, angle of attack, flight height, and backpressure. When investigating the flow laws of inlet start/unstart, an important aspect should not be neglected: that is, the nonlinear factors existing in the transition between inlet start and unstart, such as catastrophe, hysteresis, and bifurcation. From a viewpoint of nonlinearity, we have previously simulated and interpreted the nonlinear catastrophe, hysteresis, and bifurcation features of inlet start/unstart in [11]. In this paper, we will further propose a mathematical method to model the nonlinear features of inlet start/unstart. In principium, a mathematical model is a valuable way of simplifying complex data sets to represent some of the variation in the data to find patterns and trends (from which we may take a relatively simple view of the physical process of inlet start/unstart) and, by fitting mathematical theory to it, to help describe the flow laws of inlet start/unstart.

From a viewpoint of structure stability and nonlinear mathematics, this paper makes a link between the nonlinear features of inlet start/unstart and Whitney's singularity theory and, further, Thom's catastrophe theory. Starting from these internal relations, this paper makes an effort to model the nonlinear features of inlet start/unstart by the elementary catastrophe model in catastrophe theory.

II. Problems in Studying the Flow Laws of Inlet Start/Unstart

Because inlet unstart is detrimental to engine performance and may cause catastrophic damage to the engine and aircraft, the significance of studying the flow laws of inlet start/unstart may be obvious, such as for identifying and preventing inlet unstart. However, the start/unstart process is influenced by many control factors (such as flight Mach number, angle of attack, flight height, and backpressure) and, theoretically speaking, we need infinite numerical or costly experimental data to describe the flow laws of inlet start/unstart. Moreover, the flow law of inlet start/unstart is complex with

Received 4 June 2008; revision received 28 April 2009; accepted for publication 1 May 2009.

*Lecturer, School of Energy Science and Engineering; cuitao@hit.edu.cn.
†Professor, School of Energy Science and Engineering; yudaren@hcms.hit.edu.cn.
‡Lecturer, School of Energy Science and Engineering; changjuntao@hcms.hit.edu.cn.
§Professor, School of Energy Science and Engineering; baowen@hit.edu.cn.

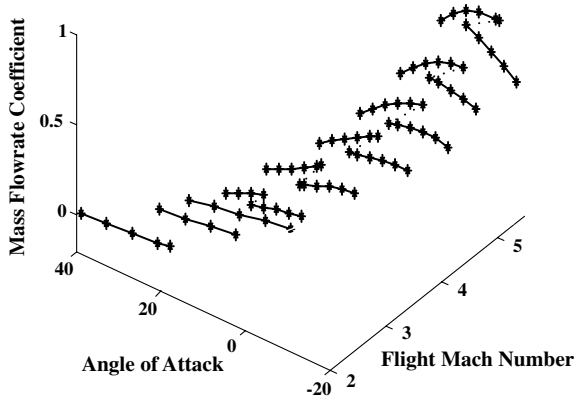

Fig. 1 Catastrophe, hysteresis, and bifurcation characteristic of inlet start/unstart.

nonlinearities such as catastrophe, hysteresis, and bifurcation, as shown in Fig. 1 [11]. The existence of hysteresis means that the catastrophe point of inlet start/unstart will be at different positions when the system operates along two adverse routes, and the existence of bifurcation means that there will be no catastrophe points under some conditions (i.e., when the inlet operates in low Mach numbers). These nonlinearity characteristics must be considered in studying the flow laws of inlet start/unstart.

III. Idea of Modeling the Catastrophe Points of Inlet Start/Unstart

As from preceding discussion, when many factors are considered, it will be very costly and difficult to describe the flow laws of inlet start/unstart simply by nearly infinite data. In this section, we will propose a new method to help study the flow laws of inlet start/unstart from the aspect of nonlinear mathematics.

A. Catastrophe Points and Singular Points

As we know, catastrophic phenomenon exists in the physical process of inlet start/unstart; the occurrence of catastrophe means the transition in the structure stability according to stability theories [12]. Mathematically, the potential function may be of great relevance for understanding the underlying dynamics. For a gradient system, its behavior can be described by the form of a mathematical function:

$$\frac{dX}{dt} = -\frac{dV(X,U)}{dX} \tag{1}$$

where X is the n-dimensional state variable or dependent variable of the system, U is the m-dimensional control variable or independent variable, t denotes time ,and V is the C^{∞}-scalar potential function. Figure 2 shows the different potential fields by changing the control parameter u of the potential function, the minimum of the function changes. The minima of the potential function are stable equilibrium points described as

$$\left\{(X,U)\left|\begin{array}{c}\partial V(X,U)/\partial X = 0\\ \partial V^2(X,U)/\partial X^2 > 0\end{array}\right.\right\} \tag{2}$$

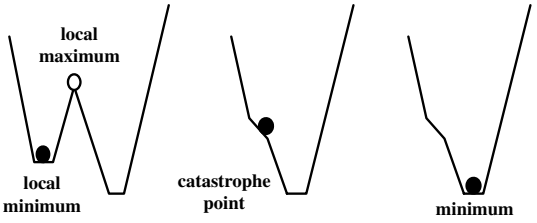

Fig. 2 Different potential fields as a result of changes in control variable u.

which are illustrated by the position of the black circle. The maxima of the potential function are unstable equilibrium points described as

$$\left\{(X,U)\left|\begin{array}{c}\partial V(X,U)/\partial X = 0\\ \partial V^2(X,U)/\partial X^2 < 0\end{array}\right.\right\} \tag{3}$$

which are illustrated by the position of the white circle. As shown in the figure, on some critical points, the smooth incremental changes in the control variable can result in a sudden jump in the state variable, and the transition is discontinuous between the two equilibrium states. The critical points are described as

$$\left\{(X,U)\left|\begin{array}{c}\partial V(X,U)/\partial X = 0\\ \partial V^2(X,U)/\partial X^2 = 0\end{array}\right.\right\} \tag{4}$$

where the Hessian determinant is zero, and the points are defined as singular points.

Mathematically, the catastrophe points of inlet start/unstart can be described by a set of singular points, and only within the neighborhood of the singular points, catastrophe can occur in the transition between inlet start and unstart. In other words, the catastrophe points have formed the catastrophe boundaries of inlet start/unstart.

B. Classification of Singular Points Under Whitney's Singularity Theory

Singular points are special points at which all the partial derivatives simultaneously vanish; it is this set of singular points that contains the significant behavior of the process. In mathematics, Whitney's singularity theory is a tool to study the singular points. It is one of the accessible entry points to both highly abstract areas of mathematics and to applied fields such as dynamical systems and bifurcations. Singularity theory solves three related key problems:

1) Given a mapping M, it determines what types of singularities any good approximation to a function f must have.

2) It tells how to perturb f slightly to obtain a nicer and simpler (but in some sense, equivalent) mapping.

3) It provides a taxonomy of singular objects and a binary key to identify them.

Hence, at the heart of singularity theory is a concept of classification [13], which is very important for the studies of singular points.

According to Whitney's singularity theory, a mapping of a surface onto a plane associates a point of the plane with each point of the surface. If a point on the surface is given coordinates (X, U) on the surface, and a point on the plane is given coordinates (Z, W), then the mapping is given by a pair of functions $Z = F(X, U)$ and $W = G(X, U)$. The mapping is said to be smooth if these functions are smooth (i.e., are differentiable for a sufficient number of times, such as polynomials). Thus, Whitney's singularity theory stated that two types of singularities (fold and cusp) are stable and persist after small deformations of the mapping.

C. Topological Method in Modeling the Singular Points Based on Thom's Catastrophe Theory

Whitney's theory gives significant information on singularities of generic mappings; this information can be used to study large numbers of diverse phenomena and processes in all areas of science, and this simple idea is the whole essence of Thom's catastrophe theory. Thom's catastrophe theory applied ideas from differential topology and topological dynamics to classification of singularities and introduced methods that described how to determine any type of singularity within a list of singularities.

In catastrophe theory, the equilibrium points of a potential function with nonzero eigenvalues of the Hessian are called Morse critical points. The Morse lemma states that at these points, the qualitative properties of the function are determined by the quadratic part of the Taylor expansion of this function. This part can be reduced to the Morse canonical form by topology transformation. If the Hessian degenerates at an equilibrium point, so that at least one of the eigenvalues is zero, the type of equilibrium point cannot be determined.

The equilibrium points of a potential function with zero eigenvalues (singular points) are also called non-Morse critical points. The core of the catastrophe theory lies in finding a canonical form for an arbitrary potential function V in a neighborhood of a non-Morse critical point. This is accomplished by conceiving suitable variable changes that render it locally possible to standardize the form of V without altering any of its qualitative properties and, in particular, its critical-point structure. Appropriate transformations are diffeomorphisms. Because a higher-order Taylor expansion is essentially needed to describe the qualitative properties, although the dimension of the variables is arbitrary, the Thom lemma states that one can split up the function in a Morse and a non-Morse part, and the latter consists of variables representing the k eigenvalues of the Hessian that become zero, and k is the codimension. The Morse part contains the n-k remaining variables. Consequently, the Hessian contains a $(n\text{-}k) \times (n\text{-}k)$ submatrix representing a Morse function. Therefore, it suffices to study the part of k variables. The canonical form of the function at the non-Morse critical point thus contains two parts: a Morse canonical form of n-k variables, in terms of the quadratic part of the Taylor series, and a non-Morse part. The latter can by put into canonical form called the *catastrophe germ* by topology transformation, which is obviously a polynomial of degree 3 or higher. Because the Morse part does not change qualitatively under small perturbations, it is not necessary to further investigate this part. The non-Morse part, however, does change. Generally, the non-Morse critical point will split into a non-Morse critical point, described by a polynomial of lower degree, and Morse critical points, or even exclusively into Morse critical points; this event is called a morsification. So the non-Morse part contains the catastrophe germ and a perturbation that controls the morsifications. Then the general form of a Taylor expansion $V(X, U)$ at a non-Morse critical point of a n-dimensional function can be written as [14]

$$V(X,U) = \mathrm{CG}(x_1, x_2, \ldots, x_k) + \mathrm{PT}(x_1, x_2, \ldots, x_k; u_1, u_2, \ldots, u_l) + \sum_{i=k+1}^{n} \varepsilon_i x_i^2 \tag{5}$$

where $\mathrm{CG}(x_1, x_2, \ldots, x_k)$ denotes the catastrophe germ, $\mathrm{PT}(x_1, x_2, \ldots, x_k; u_1, u_2, \ldots, u_l)$ denotes the perturbation germ with an m-dimensional space of parameters, l is the dimension of independent variables (corank), and in the Morse part, $\varepsilon_i = \pm 1$. In catastrophe theory, the germs with $l \leq 4$ are mathematically presented. These germs are the starting point of the infinite set of so-called simple real singularities, for which the catastrophe germs are given by the series $A_k \equiv x^{k+1}$ $(k \geq 1)$ and $D_k^{\pm} \equiv x^2 y \pm k^{k-1}$ $(k \geq 4)$. Thus, the famous "seven elementary catastrophes" are normalized to classify different singularities. In fact, these elementary catastrophes have provided certain mathematical models of the diverse catastrophe systems. These already known elementary mathematical models may help to solve the problems existing in studying the catastrophe points of inlet start/unstart. In the following section, we will try to model the catastrophe points of inlet start/unstart based on elementary catastrophe models in Thom's catastrophe theory.

IV. Modeling the Catastrophe Points of Inlet Start/Unstart

In the present study, we consider the influence of the independent variable of flight Mach number M_0 and angle of attack α on the catastrophe points of inlet start/unstart. To describe the catastrophe characteristic of inlet start/unstart, we select the mass-flow-rate coefficient Φ as the dependent variable, because there will be a catastrophic jump in the mass-flow-rate coefficient when the transition occurs between inlet start and unstart. Based on catastrophe theory, when only two variables of fight Mach number and angle of attack are considered as independent variables and mass-flow-rate coefficient is selected as a dependent variable to describe inlet start/unstart, the elementary catastrophe type of inlet start/unstart will correspondingly be described by cusp catastrophe, where $l = 1$ and $k = 2$ [11]. An introduction of cusp catastrophe is presented next.

A. Cusp Catastrophe

The cusp catastrophe, which is one of the elementary catastrophes in catastrophe theory, is the simplest discontinuous transition between two equilibrium states. Its catastrophe germ reads x^4, and the perturbation term is given by $u_1 x^2 + u_2 x$. Thus, the potential function of cusp catastrophe is described as

$$V(x, u_1, u_2) = x^4 + u_1 x^2 + u_2 x \tag{6}$$

The equilibrium surface, composed of the set of all equilibrium points, can be derived from Eq. (6) as

$$\frac{dV}{dx} = x^3 + 2u_1 x + u_2 = 0 \tag{7}$$

Then project the equilibria M into the control space by eliminating x to obtain the bifurcation line:

$$8u_1^3 + 27u_2^2 = 0 \tag{8}$$

B. Numerical Data

1. Inlet Model

Numerical data for this study were mainly provided from [11]. The overall inlet geometry is based on the similar inlet model tested within the frame of an earlier Central Institute of Aviation Motors (CIAM) and NASA flight test [15]. The computational model includes an inlet and constant-area isolator only. Figure 3 shows the geometric sketch of the inlet model. The main geometric parameters of the supersonic inlet are shown in Table 1.

2. Numerical Method

The computation is performed using the finite volume technique with upwind discretization to solve the two-dimensional compressible Reynolds-averaged Navier–Stokes equations. The air is considered to be a calorically perfect gas. The space discretization is performed by a cell-centered formulation. To account for the directed propagation of information in the inviscid part of the equations, the advection upstream splitting method (AUSM) flux vector splitting is applied for the approximation of the convective flux functions. Higher-order accuracy for the upwind discretization and consistency with the central differences used for the diffusive term is achieved by the monotonic upstream scheme for conservation-law extrapolations, and the total-variation-diminishing property of the scheme is ensured by the van Leer flux limiter. Time integration is performed by an explicit five-stage Runge–Kutta time-stepping scheme. To enhance convergence, a multigrid method, implicit residual smoothing, and local time-stepping are applied.

A renormalization group k-ε turbulence model is implemented for turbulent flows. The near-wall treatment adopts nonequilibrium wall functions, which are recommended for use in complex flows involving separation, reattachment, and impingement in which the mean flow and turbulence are subjected to severe pressure gradients and change rapidly. The supersonic inflow is defined by specifying the boundary conditions, where the definition of α is shown in Fig. 3. In the case of predominant supersonic outflow, the variables are completely extrapolated from the interior to the boundary. Otherwise, the influence of the throttle is simulated with a prescribed backpressure at the outflow boundary and the remaining variables are extrapolated. At solid walls, the no-slip boundary condition is enforced by setting the velocity components to zero. The adiabatic

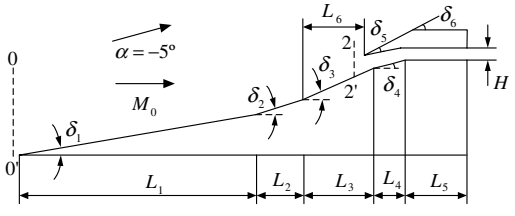

Fig. 3 Geometry sketch of the inlet model.

Table 1 Geometry parameters of supersonic inlet

Length L	L_1	L_2	L_3	L_4	L_5	L_6
Unit, m	0.267	0.068	0.085	0.035	0.095	0.074
Angle δ	δ_1	δ_2	δ_3	δ_4	δ_5	δ_6
Unit, deg	10	15	20	14	10.2	24

energy boundary condition is directly applied by zeroing the contributions of the wall faces to the dissipative fluxes.

3. Numerical Accuracy Analysis

To ensure convergence of the numerical solution, the residuals (L_2-norm) are monitored in Fig. 4. The solution can be considered as converged after approximately 3000 iterations. At this stage, the continuity residual, x-velocity residual, and energy residual reach their minimum values after falling for over 4 orders of magnitude. The turbulence residual has a 6-order-of-magnitude decrease. An additional convergence criterion enforced in this current analysis requires the difference between computed inflow and outflow mass flux to drop below 0.5%. The evaluation was performed using the coarse mesh.

The performance of a grid sensitivity analysis confirms that the grid resolution used here is sufficient to capture the physically relevant features. To ensure the accuracy of the turbulence flow solution, a value of y^+ below 5 is realized for the main portion of the wall flow region. To simulate the interaction between the shock and the boundary layer, the intersection, and reflection of the wave system, calculate the flowfield at first, and perform the technology of mesh self-adaptation based on the pressure gradient and continue to compute. In Fig. 5, the static pressure distributions along the cowl and the ramp surfaces are shown for three different grid-refinement levels: coarse (754×65), medium (1020×110), and fine (1810×205); the maximum discrepancy between the three mesh levels is less than 5%. The calculations were performed on a workstation. The CPU time needed for computation is about 1 h for the coarse mesh, 3.5 h for the medium mesh, and 9 h for the fine mesh. Out of this analysis, the medium grid was selected, and all results shown are computed applying this resolution. The use of a medium grid resolution saves the CPU time greatly.

The accuracy of the current numerical investigation is evaluated by comparison with the experimental results. The experimental data are shown in Figs. 4a and 4b in [15]. The surface pressure distributions are shown in Fig. 5, allowing for a qualitative comparison between numerical and experimental results under the freestream conditions $M_0 = 6.4$, $T_0 = 203.5$ K, and $p_0 = 3968$ Pa. Here, a discrepancy in the surface pressure distributions can be seen. Both overall pressure distributions are consistent.

4. Numerical Results of the Catastrophe Points of Inlet Start/Unstart

Using the preceding numerical methods, the numerical results of the catastrophe points of inlet start/unstart for this study have been provided in [11], as shown in Fig. 1, which shows the change of mass-flow-rate coefficient with flight Mach number and angle of attack. The simulation results are obtained by two adverse routes along the axis of angle of attack; that is, first, we increase the angle of attack gradually at a certain flight Mach number and obtain a series of simulation results, and second, we decrease the angle of attack gradually and obtain another series of simulation results. Then we project the surface in Fig. 1 into the control space spanned by flight Mach number and angle of attack to obtain the catastrophe points (bifurcation lines) of inlet start/unstart, as shown Fig. 6. The two bifurcation lines mean that there are catastrophe and hysteresis characteristics in the transitions between inlet start and unstart. Note that on certain conditions (at low Mach number), there will be no catastrophe and hysteresis. The whole phenomena mean a bifurcation.

C. Fitting Data to Cusp Catastrophe Model

1. Cobb's Estimation Theory for the Cusp Catastrophe Model

As catastrophe theory was developed as a topological theory for deterministic systems, a persistent problem with virtually all published applications has been the absence of statistical procedures for detecting the presence of a catastrophe in any given body of data. This lack has resulted in some severe criticism of catastrophe models for being, among other things, speculative and unverifiable. Thus, catastrophe models have become associated in many minds with reckless speculation and intellectual irresponsibility. As part of an effort to overcome this problem, Cobb's theory developed a stochastic catastrophe theory for fitting a catastrophe model to observed data by using stochastic differential equations [16]. In contrast to deterministic catastrophe theory, in Cobb's method of maximum likelihood estimation, stable and unstable equilibria are associated with modes and antimodes, respectively, of the system's stationary probability density function. The method is very useful for the applications of catastrophe model for many complex systems without analytical solutions.

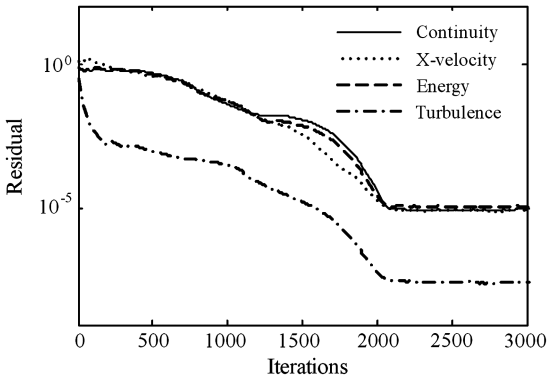

Fig. 4 Residuals for the supersonic inlet computation.

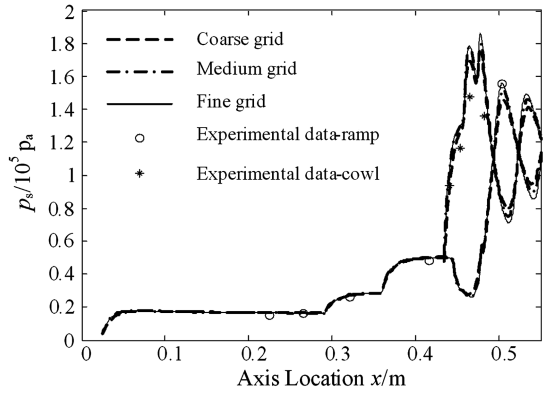

Fig. 5 Surface pressure distributions for refined grids.

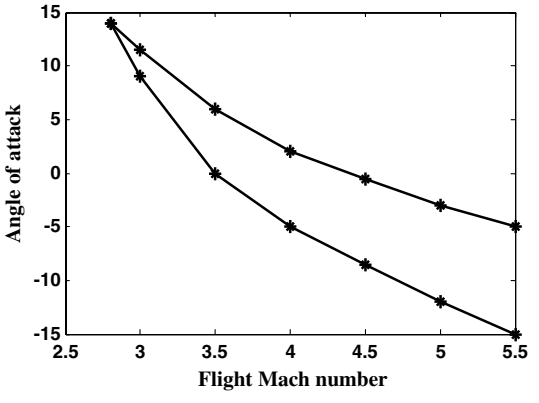

Fig. 6 Catastrophe points in the control surface of inlet start/unstart.

By using stochastic differential equations, Cobb's theory connected a probability density function $e^{-V(x)}$ to the potential function $V(x)$. For the cusp catastrophe, this becomes

$$f(x, u_1, u_2) = \xi e^{-z^4 - u_1 x^2 - u_2 x} \tag{9}$$

In Eq. (9), ξ is a constant depending on u_1 and u_2, which normalizes the probability distribution function so that it has a unit integral over its range. Equation (9) represents a cusp catastrophe model in terms of a probability density function.

Cobb's theory made the simplifying assumption that the topological transformation functions are linear of a number of independent variables in the following way, such as for the catastrophe system of inlet start/unstart:

$$x = \frac{\Phi - \lambda}{\sigma} \tag{10}$$

$$u_1 = \theta_0 + \theta_1 M_0 + \theta_2 \alpha \tag{11}$$

$$u_2 = \gamma_0 + \gamma_1 M_0 + \gamma_2 \alpha \tag{12}$$

where λ is the location parameter; σ is the scale parameter; and θ_0, θ_1, θ_2, γ_0, γ_1, and γ_2 are weights given to independent variables of M_0 and angle of attack α. These weights provide a means of evaluating each independent variable used in the model in terms of its contribution to the dependent parameter. Let likelihood function be

$$\begin{aligned} L &= L(\lambda, \sigma, \theta_0, \theta_1, \theta_2, \gamma_0, \gamma_1, \gamma_2) \\ &= \prod_{i=1}^{n} f(x_i, u_{1i}, u_{2i}; \lambda, \sigma, \theta_0, \theta_1, \theta_2, \gamma_0, \gamma_1, \gamma_2) \end{aligned} \tag{13}$$

Thus, the statistical estimation problem is to find estimates for the parameters $\hat{\lambda}$, $\hat{\sigma}$, $\hat{\theta}_0$, $\hat{\theta}_1$, $\hat{\theta}_2$, $\hat{\gamma}_0$, $\hat{\gamma}_1$, and $\hat{\gamma}_2$ that fulfills

$$L(\hat{\lambda}, \hat{\sigma}, \hat{\theta}_0, \hat{\theta}_1, \hat{\theta}_2, \hat{\gamma}_0, \hat{\gamma}_1, \hat{\gamma}_2) = \max L(\lambda, \sigma, \theta_0, \theta_1, \theta_2, \gamma_0, \gamma_1, \gamma_2) \tag{14}$$

By Cobb's estimation method, we obtain the model results (calculated bifurcation lines from the model) as shown in Fig. 7. By comparing with numerical data (simulated catastrophe points from computational fluid dynamics), it is clear that the method does not provide good results. This involves a limitation of Cobb's method: that is, the topological transformation function is linear with just a simple description of the complex topological relations between the physical system and the norm elementary catastrophe model.

2. Nonlinear Topological Transformation Method

To solve the problem, this paper puts forward a new nonlinear topological transformation method. The peculiarity of the method is about constructing nonlinear topological transformation by a neural network and applying its predominance in describing a complex nonlinear process.

To understand the following modeling idea, let us first go back to review the core of catastrophe theory; that is, the so-called catastrophe modeling is actually to find a topological transformation between the physical system and the known elementary catastrophe model. Thus, if we can set up some topological transformation function to link the catastrophe points of inlet start/unstart with the singular points set of the cusp catastrophe model, the work will be done. With this study, we divide the modeling process into three steps, and each step forms a certain topological transformation.

Considering the symmetry of the singular points set of the cusp catastrophe model as shown in Figs. 6 and 7, the first step is to construct a topological transformation by radial basis function neural network, as shown in Fig. 8, to shape the catastrophe points of inlet start/unstart into a symmetric configuration, as shown in Fig. 9. The transformation can be described as

$$\begin{cases} w_1 = M_0 \\ w_2 = NNRBF(M_0, \alpha) \end{cases} \tag{15}$$

where $NNRBF$ is the transformation function by radial basis function neural network. According to the theory of radial basis function (RBF) neural networks, the transform from the input-layer space to the hidden-layer space is nonlinear, while the transform from the hidden-layer space to the output space is linear. That is to say, the mapping between the input and output is nonlinear, and the output of the network is linear for the adjustable parameters. Then the weights of the network can be found directly by the linear equations, and so the learning speed can be quickened greatly. It can also avoid the problem of converging to local minimum. The training algorithms for an RBF neural network have been divided into two stages. First, using an unsupervised-learning algorithm, the centers for hidden-layer nodes can be determined. After the centers are fixed, the widths are determined in a way that reflects the distribution of the centers and input patterns. Once the centers and widths are fixed, the weights between the hidden and output layers can be trained.

The second step is another kind of topological transformation: smooth coordinate transformation. The coordinate system $Q(w_1, w_2)$ changes into $R(z_1, z_2)$, and this is expressed as follows:

$$\begin{cases} z_1 = l_1 w_1 + l_2 w_2 - \omega \\ z_2 = m_1 w_1 + m_2 w_2 - \upsilon \end{cases} \tag{16}$$

Here, ω and υ are the Q point value in the coordinate system $R(z_1, z_2)$, and l_1, l_2, m_1, and m_2 are the direction cosines from the coordinate system $Q(w_1, w_2)$ to the coordinate $R(z_1, z_2)$; this process is shown in Fig. 10.

The third step is an analytical topological transformation in which the target function is described as in Eq. (8) according to catastrophe theory. Let $\bar{k}$ be the absolute value of the two symmetric curves'

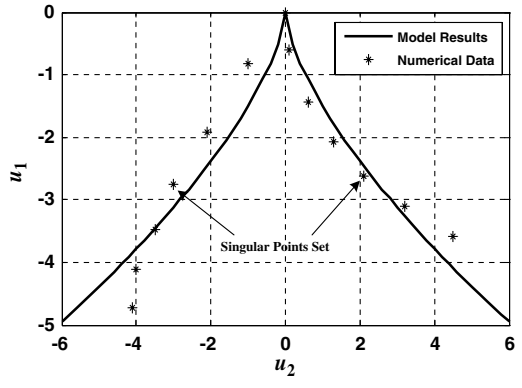

Fig. 7 Modeling the catastrophe points of inlet start/unstart by Cobb's method.

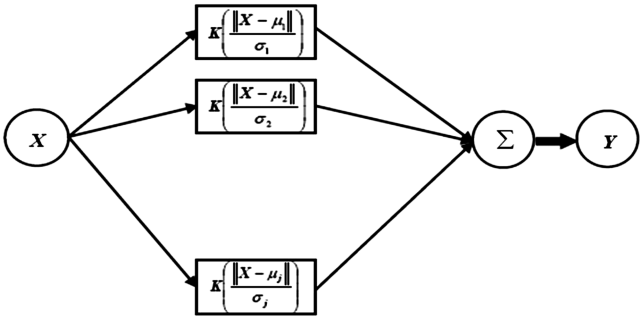

Fig. 8 Radial basis function neural network.

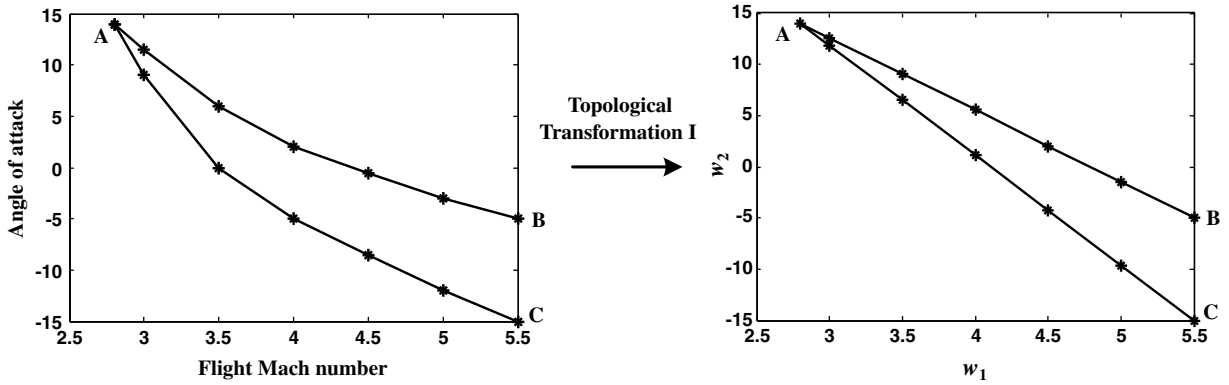

Fig. 9 Topological transformation of the first step.

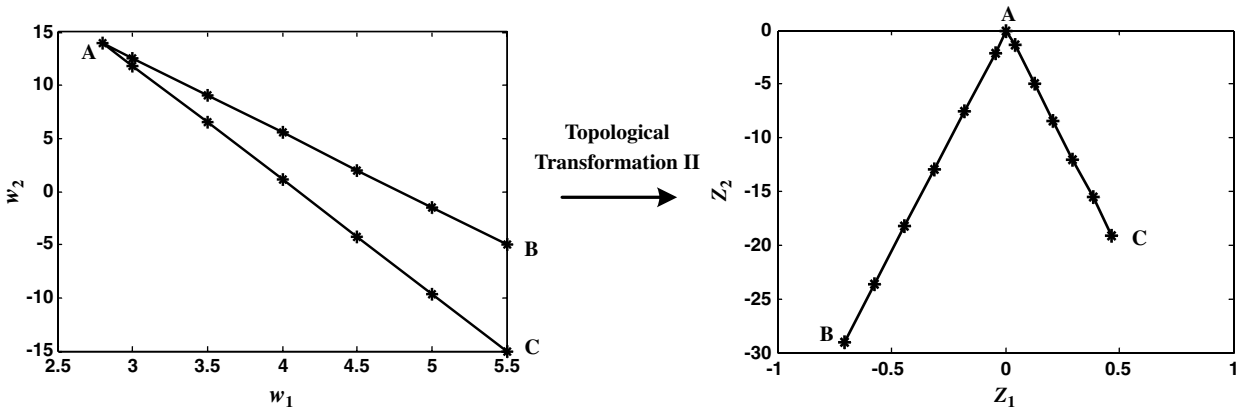

Fig. 10 Topological transformation of the second step.

approximate slope, and by constructing the following topological transformation function,

$$\begin{cases} u_1 = \sqrt[-3]{\frac{1}{8}z_2^2} \\ u_2 = \sqrt{\frac{2}{27}\bar{k}z_1} \end{cases} \tag{17}$$

we obtain the final cusp catastrophe model to describe the catastrophe points of inlet start/unstart. The model results are shown in Fig. 11, from which we can see that the model result can fit the numerical data very well. This means that the proposed method are valid in modeling the catastrophe points of inlet start/unstart and may be extended for providing mathematical description of catastrophe points of inlet start/unstart for the actual aeronautical engines such as ramjet and scramjet engines.

D. Model Test

An effective mathematical model of the catastrophe points of inlet start/unstart should be capable of not only providing accurate calculation results on the catastrophe boundaries, but also presenting effective description on the points off the catastrophe boundaries. Therefore, it is necessary to test the validity of the catastrophe model in the neighborhood of the catastrophe points. With this study, we select the origin points in the control surface of the physical system of inlet start/unstart as the test points, as shown in Fig. 12, which are denoted by $A_1, A_2, \ldots, A_5$, $B_1, B_2, \ldots, B_8$, and $C_1, C_2, \ldots, C_8$. Correspondingly, the model results in the control surface of the catastrophe model of inlet start/unstart are shown in Fig. 13, and the corresponding points are denoted by $\bar{A}_1, \bar{A}_2, \ldots, \bar{A}_5$, $\bar{B}_1, \bar{B}_2, \ldots, \bar{B}_8$, and $\bar{C}_1, \bar{C}_2, \ldots, \bar{C}_8$. Comparing the two figures, we may see that the catastrophe points in Fig. 13 (such as $\bar{A}_2$, $\bar{A}_4$, $\bar{B}_3$, $\bar{B}_6$, $\bar{C}_3$, and $\bar{C}_6$) fit

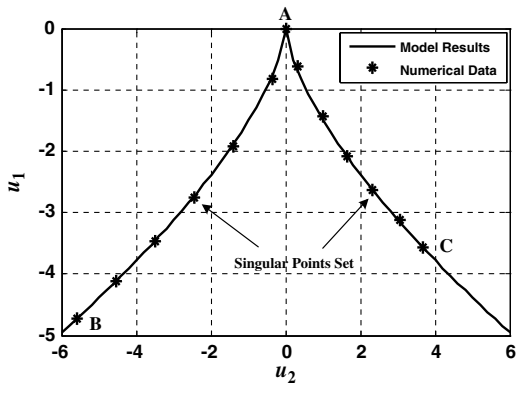

Fig. 11 Modeling the catastrophe points of inlet start/unstart by the nonlinear topological transformation method.

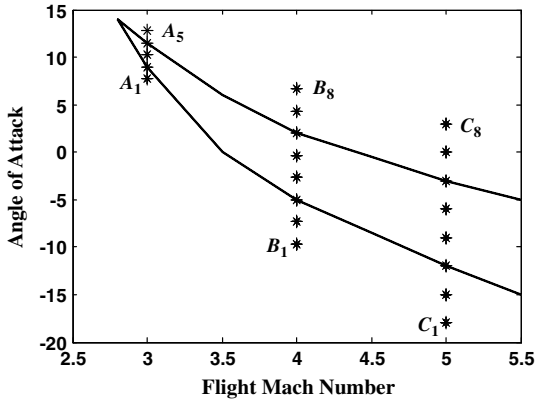

Fig. 12 Origin points in the control surface of the physical system of inlet start/unstart.

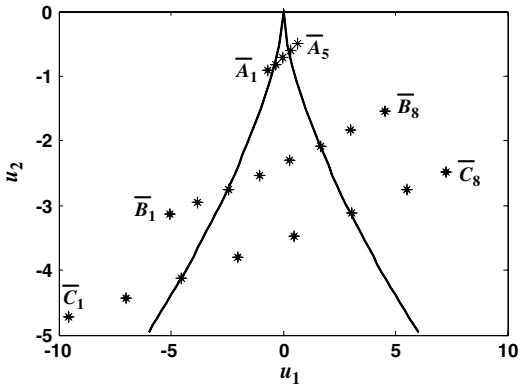

Fig. 13 Model results in the control surface of the catastrophe model of inlet start/unstart.

well with the points of A_2, A_4, B_3, B_6, C_3, and C_6, which are also the catastrophe points in Fig. 12. Geometrically, the continuous points in Fig. 12 fit well in the general direction with the points in Fig. 13, which are also continuous points, and the corresponding points in the two figures are located in the same regions divided by the curves of the catastrophe points. As described previously, these results do follow the conception of topological transformation, which is the core of catastrophe theory. Theoretically speaking, the mathematical model of the catastrophe points may provide useful nonlinear laws for identifying and preventing inlet unstart, and an example to illustrate this is from the CIAM/NASA Mach 6.5 scramjet flight test, in which it states, "although the inlet restarted at 50 seconds, the control system still identified that the inlet was unstarted for the remainder of the flight," [17] and numerical results show that "at reaching Mach 6.4 conditions, the inlet restarted but significant separation remained because of apparent hysteresis effects" [15]. This means such nonlinearities such as catastrophe and hysteresis may have influence on the identification and prevention of inlet unstart, and a mathematical model to describe the nonlinear law will be useful.

V. Conclusions

In this paper, a topological method is put forward to study the nonlinear characteristic of supersonic inlet start/unstart from a viewpoint of singular theories, and thereby a catastrophe model is set up to model the catastrophe points of inlet start/unstart. The model approach is based on nonlinear topological transformation, which has provided an improvement over the existing Cobb's method. The model has high accuracy compared with numerical data, which has primarily proven the validation of the basic ideas proposed in this paper.

Acknowledgments

The authors would like to thank Murray Tobak of NASA Ames Research Center for informative discussions, and thank the Key Program of the National Natural Science Foundation of China (No. 90816028) and the Project Supported by Development Program for Outstanding Young Teachers in Harbin Institute of Technology (HIT QNJS.2008.022) for financial support.

References

[1] Mayer, D., and Paynter, G. C., "Prediction of Supersonic Inlet Unstart Caused by Freestream Disturbances," *AIAA Journal*, Vol. 33, No. 2, 1995, pp. 266–275. doi:10.2514/3.12418

[2] Mayer, D., and Paynter, G. C., "Boundary Conditions for Unsteady Supersonic Inlet Analyses," *AIAA Journal*, Vol. 32, No. 6, 1994, pp. 1200–1206. doi:10.2514/3.12120

[3] Neaves, M. D., McRae, D. S., and Edwards, J. R., "High-Speed Inlet Unstart Calculations Using an Implicit Solution Adaptive Mesh Algorithm," AIAA Paper 2001-0825, Jan. 2001.

[4] Zha, G. C., Knight, D., and Smith, D., "Numerical Investigations of High Speed Civil Transport Inlet Unstart Transient at Angle of Attack," *Journal of Aircraft*, Vol. 35, No. 6, 1998, pp. 851–856. doi:10.2514/2.2404

[5] Zha, G. C., Knight, D., and Smith, D., "Numerical Simulation of High Speed Civil Transport Inlet Operability with Angle of Attack," *AIAA Journal*, Vol. 36, No. 7, 1998, pp. 1223–1229. doi:10.2514/2.503

[6] Cox, C., Lewis, C., and Pap, R.. "Prediction of Unstart Phenomena in Hypersonic Aircraft," AIAA Paper 1995-6018, Apr. 1995.

[7] Schmitz, D. M., and Bissinger, N. C., "Design and Testing of Fixed-Geometry Hypersonic Intakes," AIAA Paper 1998-1529, Apr. 1998.

[8] Van Wie, D. M., and Kwok, F. T., "Starting Characteristics of Supersonic Inlets," AIAA Paper 1996-2914, July 1996.

[9] Reinartz, B. U., and Herrmann, C. D., "Aerodynamic Performance Analysis of a Hypersonic Inlet Isolator Using Computation and Experiment," *Journal of Propulsion and Power*, Vol. 19, No. 5, 2003, pp. 868–875. doi:10.2514/2.6177

[10] Emami, S., and Trexler, C. A., "Experimental Investigation of Inlet-Combustor Isolators for a Dual-Mode Scramjet at a Mach Number of 4," NASA TP 3502, May 1995.

[11] Tao, C., Daren, Y., and Juntao, C., "Topological Geometry Interpretation of Hypersonic Inlet Start/Unstart Based on Catastrophe Theory," *Journal of Aircraft*, Vol. 45, No. 4, 2008, pp. 1464–1468. doi:10.2514/1.34125

[12] van der Maas, H. L. J., Kolstein, R., and van der Pligt, J., "Sudden Transitions in Attitudes," *Sociological Methods and Research*, Vol. 32, No. 2, 2003, pp. 125–152. doi:10.1177/0049124103253773

[13] Broer, H. W., Golubitsky, M., and Vegter, G., "The Geometry of Resonance Tongues: A Singularity Theory Approach," *Nonlinearity*, Vol. 16, No. 4, 2003, pp. 1511–1538. doi:10.1088/0951-7715/16/4/319

[14] Carricato, M., and Duffy, J., "Catastrophe Analysis of a Planar System with Flexural Pivots," *Mechanism and Machine Theory*, Vol. 37, No. 7, 2002, pp. 693–716. doi:10.1016/S0094-114X(02)00012-5

[15] Rodriguez, C. G., "Computational Fluid Dynamics Analysis of the Central Institute of Aviation Motors/NASA Scramjet," *Journal of Propulsion and Power*, Vol. 19, No. 4, 2003, pp. 547–555. doi:10.2514/2.6165

[16] Wagenmakers, E., "Transformation Invariant Stochastic Catastrophe Theory," *Physica D*, Vol. 211, No. 3, 2005, pp. 263–276. doi:10.1016/j.physd.2005.08.014

[17] Voland, R. T., and Auslender, A. H., "CIAM/NASA Mach 6.5 Scramjet Flight and Ground Test," AIAA Paper 1999-4848, July 1995.